RSC Advances

PAPER

View Article Online
View Journal | View Issue

Cite this: *RSC Adv.*, 2020, **10**, 42388

Functionalized heterocycle-appended porphyrins: catalysis matters†

Inna A. Abdulaeva, [a] Kirill P. Birin, *[a] Daria A. Polivanovskaia, [a] Yulia G. Gorbunova [ab] and Aslan Yu Tsivadze [ab]

The scope and limitations of the condensation of labile 2,3-diaminoporphyrin derivatives with aromatic aldehydes to provide functionalized imidazole- and pyrazine-appended porphyrins were investigated in detail. The presence of an acidic catalyst in the reaction was found to be a tool that allows the reaction path to be switched. The influence of the electronic origin of the substituents in the carbonyl components of the condensation on the yields and selectivity of the reaction was revealed. Metal-promoted cross-coupling transformations were found to be convenient for the further targeted construction of functional derivatives based on the prepared bromo-substituted pyrazinoporphyrins. Overall, these strategies provide a versatile technique for the elaboration of a variety of functionalized heterocycle-appended porphyrins for further application in the development of hybrid materials.

Received 9th October 2020
Accepted 5th November 2020

DOI: 10.1039/d0ra08603g

rsc.li/rsc-advances

Introduction

Currently, the research area of materials chemistry has attracted growing interest from scientists in various academic and applied fields since novel advanced materials are aimed to solve the scientific and technological problems in the different spheres of human life.[1–9] Among these materials, the most promising are multifunctional hybrid materials, which are characterized by a set of different properties, and thus can be applied in various fields. They can be achieved by the combination of components of diverse origin, for instance, organic and inorganic moieties.[10–14] It is worth noting that this methodology requires a detailed and comprehensive search for the mentioned components.

Porphyrins, which possess broad absorptions, and unique electrochemical and exceptional photophysical properties, have been shown to be efficient active sites for these materials for multiple applications. For example, a series of hybrid materials was constructed with tetrapyrrole active sites and inert inorganic supports for the resolution of complicated problems.[15–22]

It should be noted that solving applied problems using the material chemistry approach always requires extensive preliminary investigations. This inevitably leads to the need to elaborate novel synthetic pathways and the extension of series of known classes of macroheterocyclic compounds with optimized electronic, chemical and physicochemical properties.

In the framework of our ongoing projects, our investigations are focused on tetrapyrrolic compounds, namely porphyrins and phthalocyanines, and their synthetic modifications and search for new types of applications.[17,23–33] Recently, we developed synthetic strategies towards imidazole- and pyrazine-annulated porphyrins starting from tetrapyrrole dioxo- or diamino-derivatives and aromatic aldehydes.[28,34–38] The sterically hindered tetrapyrrole was used as a synthetic platform for the development of bifunctionalized linear and angular annulated polyaromatic compounds, water soluble derivatives for biomimetic applications and macrocycles with terminal anchoring groups.[34,38] Furthermore, the latter methodology was implemented for the elaboration of a novel class of heteroleptic sandwich-type lanthanide (porphyrinato)(phthalocyaninates)[39,40] based on heterocycle-appended porphyrin ligands.[36] In this case, the influence of the annulated N-cycle on the electronic structure of the entire molecule was revealed by UV-vis spectroscopy.

The most promising synthetic strategy giving access to porphyrins annulated with 5- and 6-membered N-heterocycles implies the use of porphyrin diamines as starting compounds. However, this approach has scarcely been studied applying only 4-bromobenzaldehyde as the carbonyl component of the condensation reaction. Meanwhile, the utilization of different substituted aldehydes allows the direct introduction of various desired functions onto the periphery of the porphyrin core. Accordingly, the scope and limitations of this condensation are of interest, especially in terms of the carbonyl reagent. Moreover, opportunities for the transformation of derivatives bearing active terminal groups are also a topic of the current investigation.

Thus, in the present work, we revealed the applicability of the mentioned synthetic approach towards heterocycle-appended porphyrins. The crucial role of the acidic catalyst in

[a]A.N. Frumkin Institute of Physical Chemistry and Electrochemistry RAS, Leninsky pr., 31, building 4, Moscow, 119071, Russia. E-mail: kirill.birin@gmail.com

[b]N.S. Kurnakov Institute of General and Inorganic Chemistry RAS, Leninsky pr., 31, Moscow, 119991, Russia

† Electronic supplementary information (ESI) available: Complete NMR characteristics of the compounds. See DOI: 10.1039/d0ra08603g

the condensation of 2,3-diaminoporphyrins with aromatic aldehydes is revealed, allowing switching of the direction of the reaction path. Further modification of the obtained heterocycle-porphyrins is shown to be efficiently achieved with the application of metal-promoted transformations. Accordingly, the functionalized imidazo- and pyrazino-porphyrins can be considered as readily available organic precursors for the elaboration of the functional hybrid materials. Consequently, molecules with functional peripheral fragments that can be converted into anchoring groups are of special interest.

Results and discussion

Previously, we reported the selective formation of imidazole-annulated derivatives upon equimolar interaction of sterically hindered nickel(II) diaminoporphyrin bearing *meso*-mesityl groups with 4-bromobenzaldehyde (Scheme 1).[35] Similar condensation with 5-fold molar excess of aldehyde decreased the selectivity of the reaction and provided a mixture of imidazo- and pyrazinoporphyrins.

In the present investigation, we chose tetrakis(4-butoxyphenyl)porphyrin as the tetrapyrrolic platform for several reasons. Firstly, the bulkiness of these aryl substituents is negligible in comparison with 2,4,6-trimethylphenyl groups, which allowed any steric effect of the *meso*-groups on the reaction course to be avoided. Next, the relatively long alkyl chain in the aromatic fragments is expected to provide sufficient solubility to all the semi-products and the final fused compounds. Finally, the electron donor effect of the alkoxy-groups is supposed to promote the condensation reaction due to the increase in the nucleophilicity of the amino-groups in the porphyrin precursor.

These peculiarities of tetrakis(4-butoxyphenyl)porphyrin have already been successfully used for the elaboration of a new class of sandwich-type complexes formed from phthalocyanine and heterocycle-appended porphyrin ligands bearing terminal reactive halogen atoms.[36] Accordingly, the extension of the series of functionalized porphyrins fused with different heterocycles is assumed to be of interest for the further design of hybrid materials based not only on porphyrin derivatives, but also on the sophisticated tetrapyrrolic polyaromatic systems.

Firstly, a series of condensations of porphyrin diamine-derivative **2** with different 4-substituted benzaldehydes was performed based on our reported methodology (Scheme 2).[35] We found that depending on the stoichiometry of the reaction and the nature of the carbonyl component, three types of compounds may form, namely, imidazoporphyrins **4**, pyrazinoporphyrins **5** and pyrazine-fused porphyrin dimer **6**. Notably, the mechanism of dimer formation, method for its targeted preparation, and complete investigation of its spectral features were reported by us previously.[28] The results of the performed series of condensation reactions are summarized in Table 1.

4-Bromobenzaldehyde (**3a**) was used as a reference aldehyde for comparison of the obtained results with the previously reported data.[35] Thus, the interaction of **2** with **3a** in a 1 : 1 molar ratio provided a mixture of **4a** and **5a** with 73% and 12% yield,

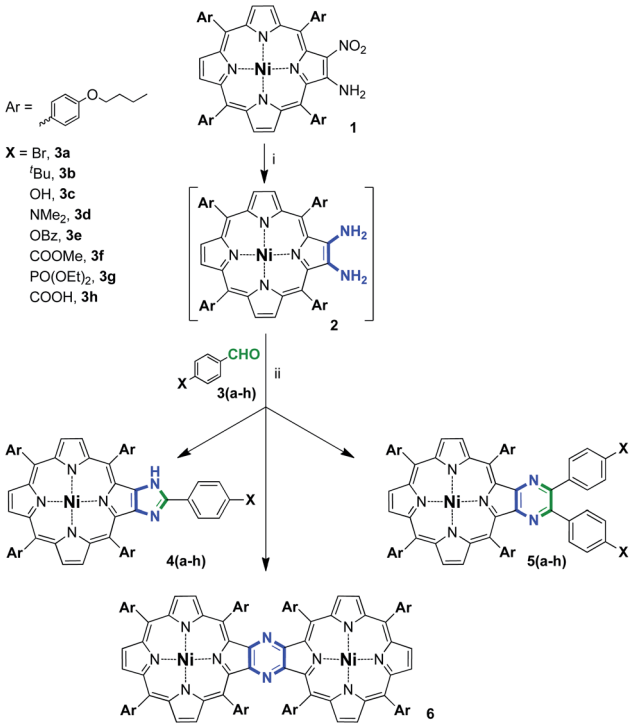

Scheme 2 Condensation of nickel(II) 2,3-diamino-tetrakis(4-butoxyphenyl)porphyrin with aromatic aldehydes. Reaction conditions: (i) $NaBH_4$, Pd/C, CH_2Cl_2/MeOH, inert atm, rt and (ii) 1,2-dichlorobenzene (DCB), 120 °C, inert atm, 18 h.

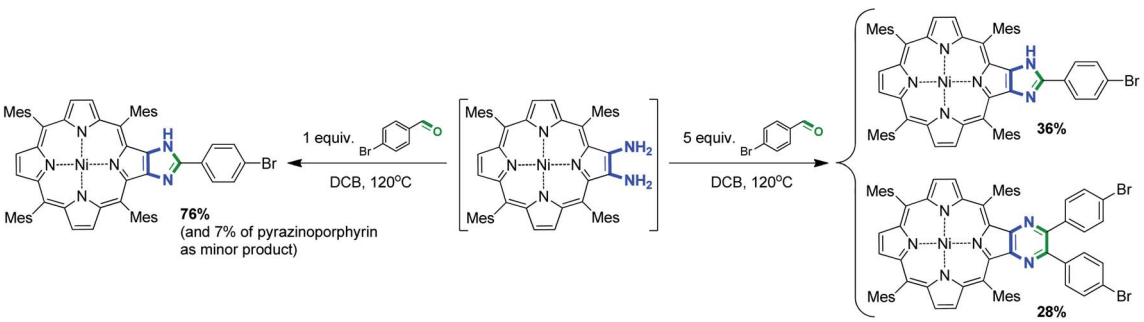

Scheme 1 Condensation of 2,3-diaminotetramesitylporphyrinato nickel(II) and 4-bromobenzaldehyde upon variation of the aldehyde ratio.[35]

Table 1 Condensation of **2** with aromatic aldehydes

Entry	Aldehyde X, (ratio)	Yields (%)	
		4	**5**[a]
1	Br, 1	73	12
2	Br, 5	—	82
3	Br, 25	—	86
4	^{t}Bu, 1	53	16
5	^{t}Bu, 5	—	78
6[b]	OH, 1	28	—
7	OH, 5	11	70
8	OBz, 1	24	73
9	OBz, 5	—	78
10	CO_2Me, 1	42	69
11	CO_2Me, 5	80	—
12	$PO(OEt)_2$, 5	60	13
13	COOH, 1	14	80
14	COOH, 5	—	82

[a] The yields of compounds are calculated based on the deficient reagent. [b] **6** was also isolated in 49% yield.

respectively (Table 1, entry 1), that is consistent with the result found for the related tetramesitylporphyrin (Scheme 1).

The designation of the yields of the reaction products in our opinion demands an additional explanation. The required aldehyde to diamine ratio for the formation of the imidazoporphyrin (1 : 1) differs from that of pyrazinoporphyrin (2 : 1). Accordingly, in the latter case, the maximum conversion of diamine that could be reached under equimolar conditions equals 1/2 of its initial quantity. This corresponds to the theoretical 100% yield of the pyrazinoporphyrin upon calculations, starting from the deficient reagent, aldehyde. In the case of imidazoporphyrin and when excess aldehyde is applied, this peculiarity of calculations disappears. Accordingly, similar speculations are valid for the calculation of the yield of **6**.

The utilization of excess 4-bromobenzaldehyde (5 equiv.) expectedly resulted in a considerable increase in the yield of pyrazinoporphyrin **5a** and complete suppression of the formation of imidazoporphyrin **4a** (Table 1, entry 2). However, a further increase in aldehyde ratio had a negligible influence on the yield of **5a** (Table 1, entry 3). It is worth noting that in the case of tetramesitylpoprhyrin, the excess aldehyde did not lead to the favorable formation of the pyrazine derivative, and both products formed in comparable yields (Scheme 1).[35] This observation can be attributed to the steric effect of the *meso*-substituents promoting the formation of a less hindered annulated compound. In contrast, the steric hindrance induced by the 4-butoxyphenyl groups is considerably less, which allows the formation of a bulkier pyrazine product.

Changing 4-bromobenzaldehyde to 4-*tert*-butylbenzaldehyde (**3b**) did not alter the selectivity of the condensation (Table 1, entry 4). Thus, the equimolar interaction provided the imidazole-fused derivative **4b** in 53% yield. The lower yield of the condensation product can be attributed to the decrease in electrophilicity of the formyl group of **3b**. The increase in the aldehyde ratio in this case also changed the reaction path to the formation of pyrazine-appended product **5b** (Table 1, entry 5).

A further increase in the electron-donor properties of the 4-substituent in the reagent and performing the condensation of porphyrin diamine **2** with 4-hydroxybenzaldehyde (**3c**) significantly altered the reaction path. Obviously, the presence of the electron-rich hydroxy-group in the reagent molecule significantly decreased the electrophilicity of the carbonyl moiety, and consequently decreased the reactivity of the aldehyde in the condensation. Thus, the interaction with a porphyrin/aldehyde ratio of 1 : 1 provided only 28% of **4c** (Table 1, entry 6). Accordingly, the majority of starting **2** did not interact with **3c** and underwent dimerization, providing **6** in 49% yield. The application of excess **3c** resulted in a decrease in the yields of **4c** and **6**, while the yield of **5c** changed drastically and reached 70% (Table 1, entry 7).

In the case of **3c**, its low reactivity also originated from the possible tautomeric enol-type transitions. Nevertheless, the alkylation of the OH-group prevented tautomerism, and thus did not allow an increase in condensed product yield. Moreover, the decrease in the reactivity of the aromatic aldehyde and the introduction of more electron-rich 4-Me_2N substituent using **3d** aldehyde completely suppressed the condensation and neither **4d** nor **5d** was detected in the reaction medium under any conditions.

The crucial influence of the electron-donating substituents in the aromatic aldehyde, and thus the electrophilicity of the

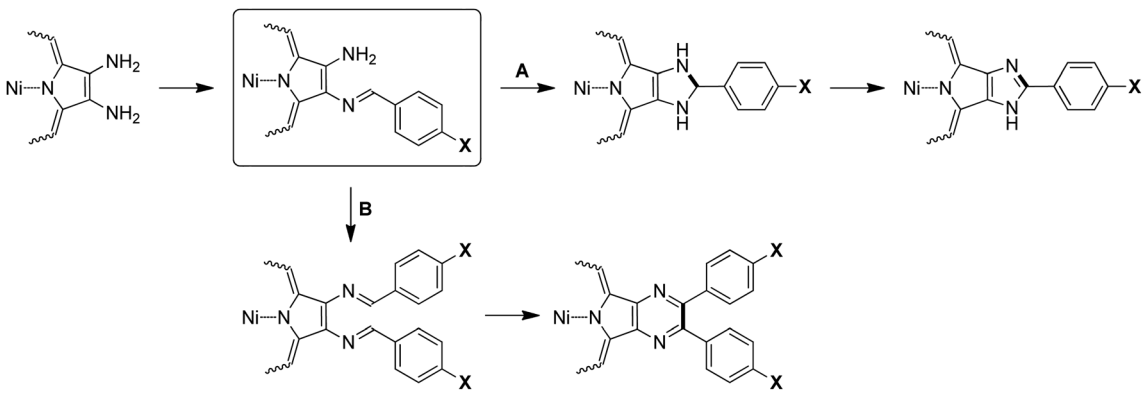

Scheme 3 Possible mechanisms for the formation of porphyrins fused with 5- and 6-membered N-heterocycles.

Table 2 Condensation of nickel(II) 2,3-diaminoporphyrinates with aromatic aldehydes in the presence of 20 mol% TsOH

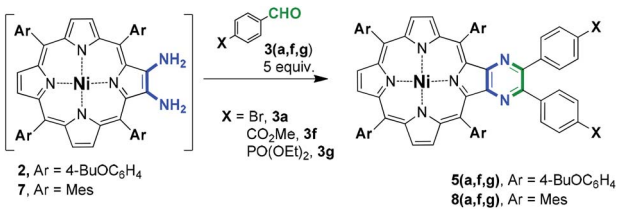

2, Ar = 4-BuOC$_6$H$_4$
7, Ar = Mes

5(a,f,g), Ar = 4-BuOC$_6$H$_4$
8(a,f,g), Ar = Mes

Entry	Porphyrin	Aldehyde	Solvent, temp. (°C)	Product, yield (%)
1	**2**	**3a**	DMF, 80	**5a**, 6[a]
2	**2**	**3a**	DCB, 100	**5a**, 64
3	**2**	**3f**	DCB, 100	**5f**, 88
4	**2**	**3g**	DCB, 100	**5g**, 42
5	**7**	**3a**	DMF, 80	**8a**, 84 (ref. 35)
6	**7**	**3a**	DCB, 100	**8a**, 66
7	**7**	**3f**	DCB, 100	**8f**, 70
8	**7**	**3g**	DCB, 100	**8g**, 48[b]

[a] 25% of **4a** and 15% of **6** were also isolated. [b] 15% of the corresponding imidazole-fused product was also isolated.

formyl group, was proven by involving 4-benzoyloxybenzaldehyde (**3e**) in the condensation (Table 1, entries 8 and 9). In this case, the electron-donating properties of the oxygen atom are diminished by the conjugation with the electron-withdrawing benzoyl fragment. Accordingly, the reactivity of **3e** was found to significantly exceed that of **3c** and its interaction with **2** in an equimolar ratio gave rise to a mixture of **4e** and **5e** (Table 1, entry 8). The increase in the aldehyde/porphyrin ratio resulted in the preferable formation of pyrazinoporphyrin **5e** with 78% yield (Table 1, entry 9).

The introduction of the electron-withdrawing groups to the benzaldehyde is obviously expected to increase the electrophilicity of the formyl moiety, and thus facilitate the condensation. Thus, the involvement of 4-methoxycarbonylbenzaldehyde (**3f**) in the condensation with **2** in an equimolar ratio provided **4f** and **5f** in high overall yield (Table 1, entry 10). Surprisingly, the increase in the ratio of **3f** resulted predominantly in the formation of **4f** with 80% yield (Table 1, entry 11). A similar effect was observed with the application of 5 equiv. of **3g** in the condensation, resulting in the formation of 60% of imidazoporphyrin **4g** together with 13% of **5g** (Table 1, entry 12).

In contrast to the 4-methoxycarbonyl- and 4-diethoxyphosphoryl derivatives, **3f** and **3g**, respectively, 4-carboxybenzaldehyde (**3h**) exhibited different reactivity. The interaction of **2** and **3f** in a 1 : 5 molar ratio smoothly provided the corresponding pyrazinoporphyrin **5f** in high yield. This specific behavior requires particular explanation, which can be provided from a mechanistic point of view.

Previously, we proposed the mechanisms for the formation of imidazo- and pyrazinoporphyrins upon condensation of a diaminoporphyrin with aromatic aldehydes.[35] The key step in both cases is the interaction of the aldehyde carbonyl group with one of the amino-groups of the porphyrin precursor (Scheme 3). However, some prerequisites have to be mentioned to analyze the further reaction steps.

The first condensation step decreases the nucleophilicity of the remaining amino-group and the electrophilicity of the CH-imine fragment in comparison with that of the starting carbonyl compound. Further, the reaction pathway is expected to be dependent on the relative reactivity of the CH-imine group and formyl group of the aldehyde. It is also reasonable to assume that the porphyrin/aldehyde ratio should affect both the first condensation step and the possible condensation with the second molecule of the aldehyde. Moreover, the preorganization of the intermediate favors the formation of a 5-membered heterocycle. The last oxidative steps of both paths are expected to be influenced similarly by the presence of electron-donor or withdrawing groups, and consequently cannot change the course of the reaction.

Thus, based on these considerations, the observed difference in the reaction paths can be explained. The electron-donor hydroxy-group causes the low reactivity of **3c** and also defines the decreased electrophilicity of the intermediate CH-imino-fragment, even in comparison with the formyl group of the aldehyde, which disfavors the intramolecular condensation (Scheme 3, path A). Accordingly, the increase in the aldehyde ratio results in the realization of path B through the kinetic facilitation of the second condensation step.

Changing the aldehyde to **3f** bearing an electron-withdrawing CO_2Me group facilitates the electrophilic steps of the reaction. In this case, the balance between paths A and B depends on the rates of all the stages. Since the intramolecular addition forming the 5-membered ring is facilitated, it can be presumed that the application of excess **3f** results in the fast formation of the imine intermediate, which further undergoes intramolecular addition and gives imidazoporphyrin **4f** as the main product. This explanation is consistent with the experiment employing **3g** in the condensation.

The surprising contrary result obtained with **3h** can be explained based another point of view. Previously, we showed that the use of a catalytic amount of acid, namely TsOH, in the condensation reaction allows the reaction pathway to be switched and the preparation of the pyrazinoporphyrin instead of imidazoporphyrin.[35] This can be achieved through the increase in its electrophilicity by the protonation equilibrium of the aldehyde carbonyl group. In the case of **3h**, the applied aldehyde contains an acidic group itself. The acidity of the aryl carboxylic acid is definitely lower than that of TsOH. Nevertheless, in the case of TsOH, only 20 mol% was sufficient for the reaction, while in the case of **3h**, the reaction mixture formally contains an equimolar amount or high excess of the acid. We suppose that this may be the reason for the reverse selectivity of the reactions in this case.

Thus, to prove this assumption, several condensation experiments were performed in the presence of a catalytic amount of TsOH (Table 2). Firstly, we attempted to involve **2** in the condensation under previously reported conditions.[35] The interaction of **2** with 5 equiv. of **3a** in DMF at 80 °C in the presence of 20 mol% of TsOH unexpectedly provided **5a** with only 6% yield and mainly the degradation of **2** was observed

(Table 2, entry 1). This behavior can be assumed to be a particular feature of the used porphyrin. Nevertheless, performing the condensation in dichlorobenzene at 120 °C successfully yielded 64% of **5a** (Table 2, entry 2). Application of these conditions in the reaction with aldehydes **3f** and **3g** also allowed the preparation of **5f** and **5g** with 88% and 42% yield (Table 2, entries 3 and 4), respectively, in contrast to Table 1, entry 12. The decrease in the yield of **5g** in the comparison with **5f** can be reasonably attributed to the partial lability of the phosphoryl moiety under the reaction conditions.

We also applied the currently found condensation conditions to the tetramesitylporphyrin to establish the influence of porphyrin type on the reaction selectivity (Table 2, entries 5 and 6). It was found that the condensation of **7** and **3a** in DCB gave rise to the pyrazine-appended porphyrin **8a** with a yield of four times less than in DMF (Table 2, compare entry 5 with entry 4). The introduction of **3f** in this reaction also allowed the preparation of pyrazinoporphyrin **8f** with high yield (Table 2, entry 7). However, the application of aldehyde **3g** led to a lower product yield (Table 2, entry 8), which can be attributed to the decreased stability of diethoxyphosphoryl aldehyde under acidic conditions. This is consistent with the results obtained for the 4-butoxyphenyl-substituted porphyrin.

Thus, based on the performed experiments summarized in Tables 1 and 2, it can be concluded that the reaction path of the condensation of 2,3-diaminoporphyrins with aromatic aldehydes strongly depends on the origin of the carbonyl component of the reaction. The selectivity of the reaction is actually a fine balance among multiple effects. Nevertheless, in most cases, a variation in the reaction conditions allowed the determination of the optimal conditions for the selective preparation of the porphyrin derivatives fused with a 5- or 6-membered N-heterocycle. The acidic catalysis was found to be a valuable tool for switching the reaction pathway to the selective formation of imidazole- or pyrazine-appended porphyrins.

The comparison of the UV-vis absorption spectra of the obtained compounds illustrates the difference in the electronic structures of the macrocycles upon fusion with 5- and 6-membered heterocycles (Fig. 1). It can be clearly seen that the imidazole-fused porphyrin **4b** demonstrates a Soret band

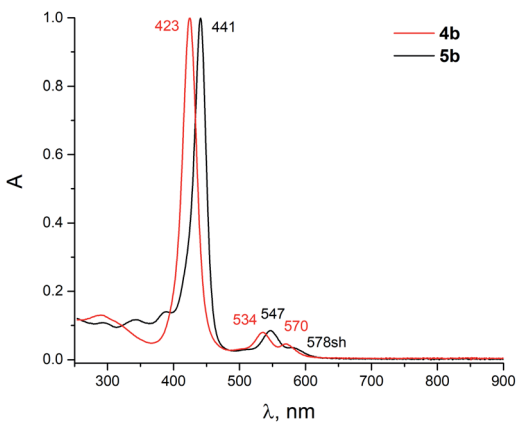

Fig. 1 UV-vis spectra of **4b** and **5b**, normalized at the Soret band ($CHCl_3$).

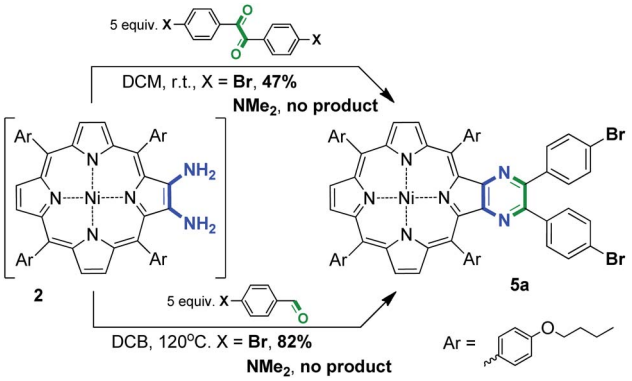

Scheme 4 Two pathways to disubstituted pyrazine-appended porphyrins.

absorption with a maximum in a typical position of 423 nm. In contrast, the fusion with a pyrazine heterocycle results in a significant change in the electronic structure of the macrocycle, as revealed the considerable red shift of the absorption bands.

Porphyrins bearing an appended diaryl-substituted pyrazine unit can be prepared *via* the interaction of 2,3-diaminoporphyrins and 4,4′-disubstituted benzils. The only reported example of this type of interaction operated with an unsubstituted benzil provided 64% yield of the target compound.[41] The main obvious disadvantage of this approach is that 4,4′-disubstituted benzils are less available in comparison with 4-substituted benzaldehydes. Nevertheless, we attempted to perform the condensation of **2** with 4,4′-dibromobenzil (Scheme 4). The interaction at ambient temperature successfully provided the desired pyrazinoporphyrin **5a**, but the obtained yield was only 47%. Moreover, this approach did not overcome the difficulty related with the preparation of fused derivatives containing electron donor groups. Accordingly, the approach with the application of functionalized aldehydes can be considered as the more preferable method.

Pyrazinoporphyrin **5a**, containing two bromo-substituents, appears to be a convenient platform for the design of highly symmetrical difunctionalized porphyrin building blocks. Moreover, recently, we demonstrated the efficient immobilization of dicarboxy-substituted pyrazinoporphyrin on the surface of the UiO-66 and UiO-67 MOFs.[42] Accordingly, we performed several metal-promoted transformations to evaluate the reactivity of bromine atoms at the appended pyrazine fragment (Scheme 5).

Firstly, the C–C-cross coupling reaction was performed with 4-methoxycarbonylphenyl pinacolborane. The interaction of the reagents in the presence of the $Pd(PPh_3)_4$/CsF catalytic system smoothly provided **9** in high yield. This approach allows the introduction of the peripheral anchoring groups and their analogues, which provides the opportunity for fine tuning the geometry of the prepared molecular building blocks related with **5h**.

The bromine atoms in **5a** also could be successfully substituted under the carbonylation conditions. Thus, the interaction of **5a** with carbon monoxide in the presence of

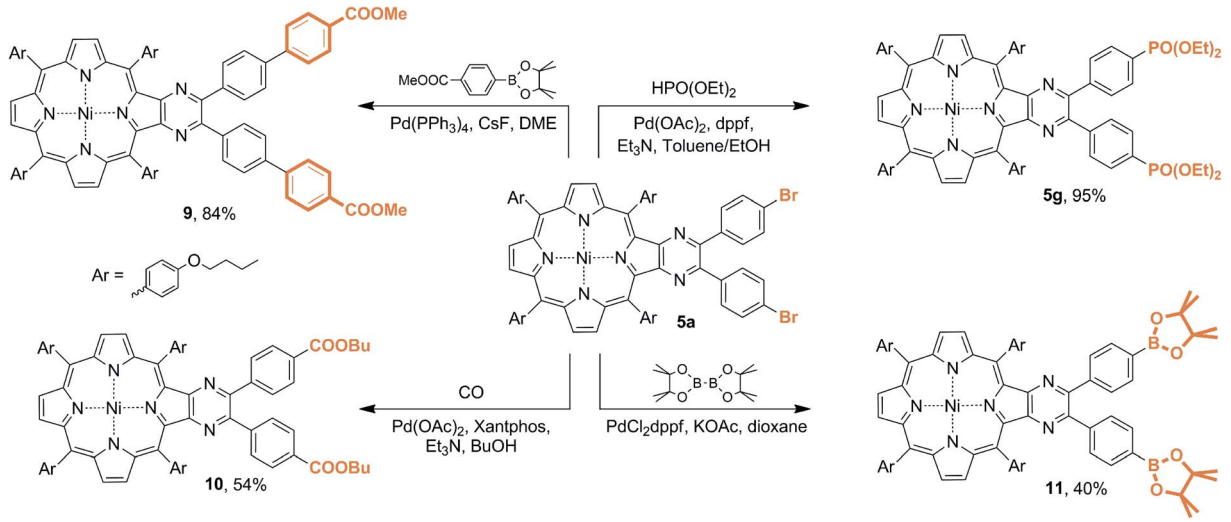

Scheme 5 Metal-promoted transformations of **5a**.

$Pd(OAc)_2$ and xantphos ligand provided double ester **10**. Despite the fact that the hydrolysis of this ester lead to **5h**, this approach simplifies the purification of the intermediate compounds, avoiding the low solubility of **5h**.

Phosphonylation of bromoarenes is another pathway for the introduction of peripheral groups capable of anchoring or providing solubilizing function. The interaction of **5a** with diethylphosphite under the reaction conditions previously found for the imidazole porphyrin derivative allowed the preparation of **5g** with virtually quantitative yield.[38,43,44] This approach appears to be more convenient than the direct synthesis of the phosphoryl-substituted pyrazine porphyrins since the corresponding aldehyde is not commercially available and has to be preliminary prepared. Moreover, its lower stability under the conditions of condensation leads to a decrease in the pyrazinoporphyrin yield, although this drawback is not peculiar to the bromo-derivative.

The substitution of bromine atoms with pinacolborane moieties allowed the preparation of **11**, which can be considered as a counterpart in the Suzuki–Miyaura cross-coupling reaction. The availability of these bromo- and boron-derivatives provided by the developed methodology opens access to a valuable class of porphyrinic platforms, which are promising for the further targeted design of functionalized derivatives for multiple applications.

The performed set of catalytic metal-promoted transformations together with that reported before[38] reveals the general paths for further modification of the imidazo- and pyrazinoporphyrins. Accordingly, these heterocyclic porphyrin derivatives can be considered as a valuable class of macrocyclic compounds suitable for the design and targeted elaboration of molecules with desired multiple functionality.

Conclusions

The expansion of the scope of the approach towards porphyrins fused with functionalized 5- and 6-membered N-heterocycles was demonstrated through the variation of the carbonyl reagent in the condensation with diaminoporphyrins. It was found that the interaction of diaminoporphyrins with 4-substituted benzaldehydes bearing electron-withdrawing groups successfully gave rise to functionalized imidazo- or pyrazino-fused derivatives, depending on the ratio of the reagents. The limitations of this transformation were also revealed. It was shown that a decrease in the electrophilicity of the formyl group in the substituted benzaldehyde suppressed the interaction with porphyrinic amino-groups. The influence of the acidic catalyst in the condensation was revealed to be a trigger to switch the direction of the reaction path.

Other approaches for the introduction of functional groups to the appended disubstituted pyrazine fragment were studied. However, the condensation of a diaminoporphyrin with 4,4′-disubstituted benzils did not reveal any valuable advantages compared to the interaction with functionalized benzaldehydes.

A series of palladium-promoted cross-coupling reactions was performed, allowing the introduction of various functional groups to the pyrazine fragment. The wide diversity of reaction types, and thus the available derivatives, makes this approach a powerful method for the elaboration of tetrapyrrolic platforms, which are promising for further applications.

Experimental

All the used reagent grade chemicals were purchased from commercial suppliers, unless otherwise stated. The solvents were purified according to conventional methods.[45] The starting 2-amino-3-nitro-tetrakis(4-butoxyphenyl)porphyrinato nickel(II) **1**,[28,36,46] 2-amino-3-nitro-tetramesitylporphyrinato nickel(II),[35] and 4-diethoxyphosphorylbenzaldehyde **3g**[44,47] were prepared following the conventional procedures. 2,3-Diamino-tetramesitylporphyrinato nickel(II) **7** was generated following the published procedure.[35] Chromatographic purification was performed using Macherey-Nagel Silica 60, 0.063–0.2 mm. Merck aluminum plates (TLC Silica 60 F254) were used for TLC analysis with hexane/dichloromethane mixtures as the eluents. Gel-permeation chromatography was performed using Bio-

Beads SX-1 sorbent (Bio-Rad) in a $CHCl_3$/EtOH (97.5 : 2.5) mixture.

MALDI-TOF mass-spectra were recorded on a Bruker Daltonics Ultraflex spectrometer in positive ions mode without a matrix. UV-vis spectra were recorded on a Unicam UV-4 spectrophotometer in rectangular quartz cells with an optical path of 0.1–10 mm in the range of 250–900 nm. ^{1}H NMR spectra were recorded on a Bruker Avance III spectrometer with 600 MHz proton frequency in $CDCl_3$ or a mixture of $CDCl_3$/MeOD at ambient temperature with the use of the residual solvent resonance as the internal reference. The complete NMR spectra are presented in the ESI.†

4-Benzoyloxybenzaldehyde 3e

4-Hydroxybenzaldehyde (4 g, 32.7 mmol) was dissolved in DCM (30 mL) under argon and Et_3N (4.6 mL, 32.7 mmol) was added. The solution was cooled in ice bath to ~0 °C and a solution of BzCl (4.00 g, 32.7 mmol) in DCM (10 mL) was added dropwise with stirring. The resulting mixture was stirred at 0 °C for 3 h. Afterwards the reaction mixture was washed with water (2 × 50 mL), dried over Na_2SO_4 and evaporated to give a pale solid (6.543 g, 88%).

^{1}H NMR ($CDCl_3$; δ, ppm; J, Hz): 10.05 (s, 1H, CHO), 8.23 (d, 2H, $^3J = 7.7$, $CH_{o\text{-Bz}}$), 8.00 (d, 2H, $^3J = 8.2$, $CH_{m\text{-Ar}}$), 7.69 (t, 1H, $^3J = 7.5$, $CH_{p\text{-Bz}}$), 7.56 (d, 2H, $^3J = 7.7$, $CH_{m\text{-Bz}}$), 7.44 (d, 2H, $^3J = 8.3$, $CH_{o\text{-Ar}}$).

^{13}C NMR ($CDCl_3$; δ, ppm): 191.07 (CHO), 164.66 (C=O), 155.88 (C–O), 134.27 (C–CHO), 134.18 ($CH_{p\text{-Bz}}$), 131.43 ($CH_{o\text{-Ar}}$), 130.44 ($CH_{o\text{-Bz}}$), 129.11 ($CH_{m\text{-Bz}}$), 128.88 (C–C=O), 122.70 ($CH_{m\text{-Ar}}$).

4-Methoxycarbonylphenyl pinacolborane

4-Methoxycarbonylphenyl boronic acid (900 mg, 5 mmol) and pinacol (708 mg, 6 mmol) were refluxed in freshly distilled THF (15 mL) under an argon atmosphere for 6 h. Afterwards, the reaction mixture was cooled to ambient temperature, diluted with EtOAc (20 mL) and extracted with water (3 × 20 mL). The organic phase was evaporated to provide the target compound as a white solid (1.26 g, 96%).

^{1}H NMR ($CDCl_3$; δ, ppm; J, Hz): 8.02 (d, 2H, $^3J = 7.8$, o-CH_{Ar}), 7.87 (d, 2H, $^3J = 7.8$, m-CH_{Ar}), 3.92 (s, 3H, $COOCH_3$), 1.35 (s, 12H, CH_{3Pin}).

^{13}C NMR ($CDCl_3$; δ, ppm): 167.30 (C=O), 134.81 (CH_{Ar}), 132.47 (C–CO), 128.74 (CH_{Ar}), 84.32 (C_{Pin}), 52.21 (OCH_3), 25.02 (CH_{3Pin}). The resonance of C–B_{pin} was not observed.

General procedure 1

The preparation of 2,3-diaminoporphyrins. In a typical experiment, 2-amino-3-nitroporphyrin (0.05 mmol) was dissolved in a mixture of freshly distilled dry DCM (16 mL) and MeOH (0.6 mL). The resulting solution was purged with argon, and 10% Pd/C (25 mg) was added upon vigorous stirring. Afterwards, $NaBH_4$ (28 mg, 0.75 mmol) was added and the mixture was stirred at ambient temperature for *ca.* 15 min until complete consumption of the starting material was observed by TLC (silica gel, DCM/hexane = 2 : 1). After complete reduction, the mixture was filtered through Celite-545 under an argon atmosphere, the obtained solution was immediately evaporated *in vacuo*, and the obtained 2,3-diaminoporphyrin was employed in the subsequent reaction without purification and characterization because of its high susceptibility to oxidation.

General procedure 2

The condensation of 2,3-diaminoporphyrins with aromatic aldehydes under catalyst-free conditions. The freshly prepared 2,3-diaminoporphyrin (0.05 mmol) was dissolved under argon in dry dichlorobenzene (DCB) (8 mL) and the required amount of the aromatic aldehyde was added (Table 1). The obtained solution was heated at 120 °C under an argon atmosphere overnight. After the complete consumption of diamine according to TLC, the reaction mixture was evaporated to dryness and the residue was applied to a column packed with silica gel in hexane. The column was eluted with hexane/DCM mixtures (0 → 100% of DCM) and further with DCM/MeOH mixtures (0 → 5% of MeOH) depending on the polarity of the functional groups in the appended heterocyclic fragment. The isolated yields of the annulated compounds are summarized in Table 1.

General procedure 3

The condensation of 2,3-diaminoporphyrins with aromatic aldehydes under acid catalyzed conditions. The condensation and treatment of the reaction mixture were generally the same as that described in general procedure **2**. The difference is the addition of 20 mol% (based on the amount of the 2-amino-3-nitroporphyrin in the reduction) of TsOH before heating of the reaction mixture and reaction temperature of 100 °C. The isolated yields of the condensed products are summarized in Table 2.

4a

^{1}H NMR ($CDCl_3$; δ, ppm; J, Hz): 8.84–8.79 (m, 4H, H_β), 8.77 (d, 1H, $^3J = 4.9$, H_β), 8.76 (d, 1H, $^3J = 4.9$, H_β), 8.65 (s, 1H, NH), 7.98 (d, 2H, $^3J = 8.2$, $CH_{o\text{-Ar}}$), 7.95 (d, 2H, $^3J = 8.2$, $CH_{o\text{-Ar}}$), 7.91 (d, 4H, $^3J = 6.4$, $CH_{o\text{-Ar}}$), 7.65 (d, 2H, $^3J = 8.2$, o-CH), 7.59 (d, 2H, $^3J = 8.2$, m-CH), 7.35 (d, 2H, $^3J = 8.2$, $CH_{m\text{-Ar}}$), 7.28 (d, 2H, $^3J = 8.2$, $CH_{m\text{-Ar}}$), 7.20 (d, 4H, $^3J = 8.2$, $CH_{m\text{-Ar}}$), 4.27 (t, 4H, $^3J = 6.5$, CH_2O), 4.20 (t, 4H, $^3J = 6.5$, CH_2O), 2.04–1.89 (m, 8H, CH_2), 1.74–1.60 (m, 8H, CH_2), 1.06–1.15 (m, 12H, CH_3).

^{13}C NMR ($CDCl_3$; δ, ppm): 159.76, 159.23, 159.14, 151.95, 150.62, 144.38, 142.58, 142.44, 142.31, 141.77, 141.66, 139.17, 134.88, 134.81, 134.78, 133.79, 133.17, 133.13, 132.94, 132.74, 132.31, 132.26, 131.87, 131.81, 131.64, 131.48, 129.95, 129.84, 127.33, 126.83, 123.50, 119.67, 119.59, 116.12, 114.36, 113.58, 113.30, 113.07, 68.42, 68.11, 31.70, 31.67, 31.54, 19.58, 19.55, 14.13, 14.10, 14.09.

MALDI-TOF MS: m/z calcd for $C_{67}H_{63}BrN_6NiO_4$ $[M]^+$ 1152.34, found 1152.25.

UV-vis ($CHCl_3$; λ_{max}, nm (log ε)): 308 (4.51), 422 (5.37), 534 (4.28), 569 (4.05).

4b

^{1}H NMR ($CDCl_3$; δ, ppm; J, Hz): 8.82 (s, 2H, H_β), 8.79 (s, 2H, H_β), 8.76 (d, 1H, $^3J = 4.9$, H_β), 8.75 (d, 1H, $^3J = 5.0$, H_β), 8.67 (s, 1H, NH), 7.99 (d, 2H, $^3J = 8.1$, $CH_{o\text{-Ar}}$), 7.97 (d, 2H, $^3J = 7.9$, $CH_{o\text{-Ar}}$), 7.91 (d, 4H, $^3J = 8.2$, $CH_{o\text{-Ar}}$), 7.74 (d, 2H, $^3J = 8.0$, *o*-CH), 7.50 (d, 2H, $^3J = 8.0$, *m*-CH), 7.37 (d, 2H, $^3J = 8.0$, $CH_{m\text{-Ar}}$), 7.28 (d, 2H, $^3J = 8.2$, $CH_{m\text{-Ar}}$), 7.20 (d, 4H, $^3J = 8.1$, $CH_{m\text{-Ar}}$), 4.33–4.25 (m, 4H, CH_2O), 4.21 (t, 4H, $^3J = 6.5$, CH_2O), 2.05–1.97 (m, 4H, CH_2), 1.97–1.90 (m, 4H, CH_2), 1.75–1.60 (m, 8H, CH_2), 1.39 (s, 9H, ^{t}Bu), 1.16–1.10 (m, 6H, CH_3), 1.09 (t, 6H, $^3J = 7.4$, CH_3).

^{13}C NMR ($CDCl_3$; δ, ppm): 159.74, 159.19, 159.12, 152.75, 152.05, 151.95, 144.42, 142.59, 142.33, 142.22, 141.68, 141.55, 139.05, 134.96, 134.80, 133.81, 133.27, 132.87, 132.63, 132.38, 131.75, 131.69, 131.62, 129.91, 128.13, 127.10, 126.03, 125.81, 119.52, 119.42, 116.17, 114.37, 113.52, 113.33, 113.06, 68.40, 68.12, 31.73, 31.68, 31.58, 31.38, 29.85, 19.56, 14.11.

MALDI-TOF MS: m/z calcd for $C_{71}H_{72}N_6NiO_4$ $[M]^+$1130.50, found 1130.59.

UV-vis ($CHCl_3$; λ_{max}, nm; log(ε)): 289 (4.54), 423 (5.36), 534 (4.32), 570 (4.06).

4c

^{1}H NMR ($CDCl_3$; δ, ppm; J, Hz): 8.86–8.72 (br.m, 6H, H_β), 8.55 (br.s, 1H, NH), 7.96 (br.s, 4H, $CH_{o\text{-Ar}}$), 7.91 (d, 4H, $^3J = 8.1$, $CH_{o\text{-Ar}}$), 7.62 (d, 2H, $^3J = 8.2$, *o*-CH), 7.32 (br.s, 4H, $CH_{m\text{-Ar}}$), 7.19 (d, 4H, $^3J = 8.2$, $CH_{m\text{-Ar}}$), 6.83 (d, 2H, $^3J = 8.1$, *m*-CH), 4.23 (t, 4H, $^3J = 6.5$, CH_2O), 4.20 (t, 4H, $^3J = 6.5$, CH_2O), 1.98–1.90 (m, 8H, CH_2), 1.68–1.59 (m, 8H, CH_2), 1.11–1.04 (m, 12H, CH_3).

Satisfactory ^{13}C NMR spectrum was not obtained for **4c** as a result of broadening of the most of its signals. The acquired spectrum is presented in the ESI.†

MALDI-TOF MS: m/z calcd for $C_{67}H_{64}N_6NiO_5$ $[M]^+$ 1090.43, found m/z 1090.43.

UV-vis ($CHCl_3$; λ_{max}, nm (log ε)): 281 (4.49), 421 (5.38), 534 (4.26), 570 (4.00).

4e

^{1}H NMR ($CDCl_3$; δ, ppm; J, Hz): 8.85–8.79 (m, 4H, H_β), 8.79–8.74 (m, 2H, H_β), 8.70 (s, 1H, NH), 8.26 (d, 2H, $^3J = 7.6$, $CH_{o\text{-Bz}}$), 8.03–7.96 (m, 4H, $CH_{o\text{-Ar}}$) 7.92 (d, 4H, $^3J = 8.1$, $CH_{o\text{-Ar}}$), 7.86 (d, 2H, $^3J = 8.2$, *o*-CH), 7.68 (t, 1H, $^3J = 7.6$, $CH_{p\text{-Bz}}$), 7.56 (t, 2H, $^3J = 7.6$, $CH_{m\text{-Bz}}$), 7.38 (d, 2H, $^3J = 8.0$, $CH_{m\text{-Ar}}$), 7.34 (d, 2H, $^3J = 8.3$, o-CH_{Ar}), 7.29 (d, 2H, $^3J = 8.1$, $CH_{m\text{-Ar}}$), 7.21 (d, 4H, $^3J = 8.1$, $CH_{m\text{-Ar}}$), 4.32–4.25 (m, 4H, CH_2O), 4.21 (t, 4H, $^3J = 6.5$, CH_2O), 2.03–1.96 (m, 4H, CH_2), 1.94 (quint, 4H, $^3J = 6.5$, CH_2), 1.72–1.60 (m, 8H, CH_2) 1.15–1.06 (m, 12H, CH_3).

^{13}C NMR ($CDCl_3$; δ, ppm): 165.04, 159.67, 159.10, 159.01, 151.89, 151.77, 150.92, 144.28, 142.50, 142.28, 142.15, 141.62, 141.51, 139.09, 134.80, 134.68, 133.81, 133.67, 133.10, 133.02, 132.79, 132.57, 132.23, 131.69, 131.64, 131.51, 131.46, 130.30, 129.84, 129.42, 128.69, 128.62, 127.10, 126.84, 122.35, 119.48, 119.40, 116.04, 114.25, 113.48, 113.20, 112.94, 68.29, 68.00, 31.55, 31.44, 19.43, 13.98.

MALDI-TOF MS: m/z calcd for $C_{74}H_{68}N_6NiO_6$ $[M]^+$ 1194.46, found m/z 1194.50.

UV-vis ($CHCl_3$; λ_{max}, nm (log ε)): 312 (*4.70*), *422* (*5.65*), *534* (*4.54*), *571* (*4.28*).

4f

^{1}H NMR ($CDCl_3$; δ, ppm; J, Hz): 8.84–8.79 (m, 4H, H_β), 8.78–8.74 (m, 3H, H_β + NH), 8.12 (d, 2H, $^3J = 8.0$, CH_{Ar}), 7.98 (d, 2H, $^3J = 8.4$, CH_{Ar}), 7.97 (d, 2H, $^3J = 8.4$ Hz, CH_{Ar}), 7.91 (br.d, 4H, $^3J = 8.4$, CH_{Ar}), 7.84 (d, 2H, $^3J = 8.0$, CH_{Ar}), 7.38 (d, 2H, $^3J = 8.1$, $CH_{m\text{-Ar}}$), 7.29 (d, 2H, $^3J = 8.1$, $CH_{m\text{-Ar}}$), 7.20 (d, 4H, $^3J = 8.1$, $CH_{m\text{-Ar}}$), 4.32–4.26 (m, 4H, CH_2O), 4.20 (br.t, 4H, $J = 5.8$ Hz, CH_2O), 3.98 (s, 3H, $COOCH_3$), 2.05–1.97 (m, 4H, CH_2), 1.94 (quint., 4H, $^3J = 6.8$, CH_2), 1.74–1.61 (m, 8H, CH_2), 1.14 (t, 3H, $^3J = 7.4$, CH_3), 1.13 (t, 3H, $^3J = 7.4$, CH_3), 1.09 (t, 6H, $^3J = 7.4$, CH_3).

^{13}C NMR ($CDCl_3$; δ, ppm): 166.76, 159.83, 159.29, 159.16, 152.11, 150.41, 144.39, 142.58, 142.49, 142.33, 141.80, 141.70, 139.38, 134.87, 134.80, 133.79, 133.14, 133.08, 132.98, 132.79, 132.25, 131.91, 131.84, 131.66, 131.48, 130.49, 130.39, 129.97, 126.75, 125.60, 119.73, 119.68, 116.13, 114.42, 113.67, 113.34, 113.08, 68.47, 68.15, 68.12, 52.39, 31.71, 31.67, 31.56, 19.60, 19.57, 19.55, 14.14, 14.10.

MALDI-TOF MS: m/z calcd for $C_{69}H_{66}N_6NiO_6$ $[M]^+$ 1132.44, found 1132.36.

UV-vis ($CHCl_3$; λ_{max}, nm (log ε)): 328 (4.42), 424 (5.35), 534 (4.25), 570 (3.98).

4g

^{1}H NMR ($CDCl_3$; δ, ppm; J, Hz): 8.88–8.81 (br.m, 4H, H_β), 8.79 (br.s, 3H, H_β + NH), 8.00 (d, 4H, $^3J = 8.2$, $CH_{o\text{-Ar}}$), 7.97–7.88 (m, 8H, $CH_{o\text{-Ar}}$ + *o*- and *m*-CH) 7.41 (br.d, 2H, $^3J = 7.9$, $CH_{m\text{-Ar}}$), 7.31 (br.d, 2H, $^3J = 8.1$, $CH_{m\text{-Ar}}$), 7.23 (d, 4H, $^3J = 8.2$, $CH_{m\text{-Ar}}$), 4.35–4.28 (br.m, 4H, CH_2O), 4.23 (t, 4H, $^3J = 6.6$, CH_2O), 4.25–4.12 (m, 4H, $CH_3C\underline{H}_2O$), 2.03 (br.s, 4H, CH_2), 1.97 (quint, 4H, $^3J = 6.7$, CH_2), 1.76–1.70 (br.m, 4H, CH_2), 1.66 (sext, 4H, $^3J = 7.5$, CH_2), 1.40 (t, 6H, $^3J = 7.1$, $C\underline{H}_3CH_2O$), 1.19–1.13 (br.m, 6H, CH_3), 1.11 (t, 6H, $^3J = 7.4$, CH_3).

^{13}C NMR ($CDCl_3$; δ, ppm): 159.72, 159.15, 159.04, 151.94, 150.19, 144.26, 142.45, 142.37, 142.21, 141.68, 141.58, 139.24, 134.74, 134.67, 134.37 (d, $^1J_{C-P} = 3.2$ Hz), 133.66, 133.01, 132.96, 132.87, 132.67, 132.53, 132.47, 132.14, 131.80, 131.73, 131.53, 131.34, 129.85, 129.56, 128.30, 126.61, 125.62, 125.52, 119.59 (d, $^2J_{C-P} = 7.5$ Hz), 115.99, 114.28, 113.54, 113.21, 112.96, 68.35, 68.00, 62.30 (d, $^2J_{C-P} = 5.3$ Hz), 31.59, 31.55, 31.44, 19.46, 19.42, 16.38 (d, $^3J_{C-P} = 6.4$ Hz), 14.01, 13.97.

^{31}P NMR ($CDCl_3$; δ, ppm): 18.04 (s).

MALDI-TOF MS: m/z calcd for $C_{71}H_{73}N_6NiO_7P$ $[M]^+$ 1210.46, found 1210.27.

UV-vis ($CHCl_3$; λ_{max}, nm (log ε)): 319 (4.51), 424 (5.43), 534 (4.32), 569 (4.05).

4h

^{1}H NMR (20% MeOD in $CDCl_3$; δ, ppm; J, Hz): 8.71–8.66 (br.s, 4H, H_β), 8.64 (s, 2H, H_β), 8.04 (d, 2H, $^3J = 8.0$, *m*-CH), 7.86 (d, 4H, $^3J = 8.1$, $CH_{o\text{-Ar}}$), 7.79 (d, 4H, $^3J = 8.2$, $CH_{o\text{-Ar}}$), 7.75 (d, 2H, $^3J = 8.0$, *o*-CH), 7.27 (br.s, 2H, $CH_{m\text{-Ar}}$), 7.18 (br.s, 2H, $CH_{m\text{-Ar}}$), 7.09 (d, 4H, $^3J = 8.2$, $CH_{m\text{-Ar}}$), 4.18 (br.t, 4H, $^3J = 6.5$, CH_2O), 4.10 (t, 4H, $^3J = 6.5$, CH_2O), 1.93–1.85 (br.m, 4H, CH_2), 1.82 (quint, 4H,

^3J = 6.5, CH_2), 1.57 (sext, 4H, ^3J = 7.6, CH_2), 1.52 (sext, 4H, ^3J = 7.5, CH_2), 1.01 (t, 6H, ^3J = 7.4, CH_3), 0.97 (t, 6H, ^3J = 7.4, CH_3).

^{13}C NMR (20% MeOD in $CDCl_3$; δ, ppm): 168.28, 158.93, 150.54, 142.23, 141.54, 134.59, 134.52, 133.66, 132.97, 132.67, 131.64, 130.86, 130.44, 125.54, 119.49, 114.21, 113.19, 112.91, 68.00, 31.42, 19.31, 19.29, 13.76.

MALDI-TOF MS: m/z calcd for $C_{68}H_{64}N_6NiO_6$ $[M]^+$ 1118.42, found 1117.90.

UV-vis ($CHCl_3$; λ_{max}, nm (log ε)): 329 (4.32), 425 (5.13), 534 (4.15), 569 (3.90).

5a

^{1}H NMR ($CDCl_3$; δ, ppm; J, Hz): 8.86 (d, 2H, ^3J = 4.9, H_β), 8.76 (d, 2H, ^3J = 4.9, H_β), 8.72 (s, 2H, H_β), 7.88 (d, 4H, ^3J = 8.5, $CH_{o\text{-}Ar}$), 7.79 (d, 4H, ^3J = 8.5, $CH_{o\text{-}Ar}$), 7.41 (d, 4H, ^3J = 8.5, o-CH), 7.30 (d, 4H, ^3J = 8.4, m-CH), 7.20 (d, 4H, ^3J = 8.6, $CH_{m\text{-}Ar}$), 7.18 (d, 4H, ^3J = 8.5, $CH_{m\text{-}Ar}$), 4.23–4.16 (m, 8H, CH_2O), 2.02 (quint, 4H, ^3J = 6.6, CH_2), 1.94 (quint, 4H, ^3J = 6.6, CH_2), 1.72 (sext, 4H, ^3J = 6.6, CH_2), 1.64 (sext, 4H, ^3J = 6.6, CH_2), 1.15 (t, 6H, ^3J = 7.4, CH_3), 1.09 (t, 6H, ^3J = 7.4, CH_3).

^{13}C NMR ($CDCl_3$; δ, ppm): 159.39, 159.29, 147.57, 144.18, 142.79, 142.01, 138.37, 134.75, 134.28, 133.03, 132.93, 132.62, 132.30, 132.12, 131.66, 131.24, 123.41, 120.55, 116.55, 113.24, 113.16, 68.15, 68.13, 31.90, 31.66, 19.78, 19.55, 14.23, 14.10.

MALDI-TOF MS: m/z calcd for $C_{74}H_{66}Br_2N_6NiO_4$ $[M]^+$ 1318.29, found 1318.08.

UV-vis ($CHCl_3$; λ_{max}, nm (log ε)): 347 (4.30), 403sh (4.42), 447 (5.10), 551 (4.10), 581sh (3.69).

5b

^{1}H NMR ($CDCl_3$; δ, ppm; J, Hz): 8.82 (d, 2H, ^3J = 4.9, H_β), 8.75 (d, 2H, ^3J = 4.9, H_β), 8.71 (s, 2H, H_β), 7.89 (d, 4H, ^3J = 8.2, $CH_{o\text{-}Ar}$), 7.83 (d, 4H, ^3J = 8.1, $CH_{o\text{-}Ar}$), 7.43 (d, 4H, ^3J = 8.1, o-CH), 7.27 (d, 4H, ^3J = 8.3, m-CH), 7.23 (d, 4H, ^3J = 8.2, $CH_{m\text{-}Ar}$), 7.20 (d, 4H, ^3J = 8.2, $CH_{m\text{-}Ar}$), 4.26 (t, 4H, ^3J = 6.5, CH_2O), 4.20 (t, 4H, ^3J = 6.5, CH_2O), 2.04 (quint, ^3J = 6.6, 4H, CH_2), 1.93 (quint, 4H, ^3J = 6.7, CH_2), 1.72 (sext, 4H, ^3J = 7.4, CH_2), 1.64 (sext, 4H, ^3J = 7.4, CH_2), 1.37 (s, 18H, ^{t}Bu), 1.14 (t, 6H, ^3J = 7.4, CH_3), 1.09 (t, 6H, ^3J = 7.4, CH_3).

^{13}C NMR ($CDCl_3$; δ, ppm): 159.30, 159.23, 151.74, 148.78, 147.35, 144.29, 142.55, 141.71, 136.88, 134.74, 134.37, 133.44, 132.85, 132.77, 132.75, 131.86, 131.60, 130.40, 124.72, 120.31, 116.33, 113.20, 113.15, 68.13, 68.10, 32.04, 31.67, 31.46, 19.82, 19.55, 14.24, 14.10.

MALDI-TOF MS: m/z calcd for $C_{82}H_{84}N_6NiO_4$ $[M]^+$ 1274.59, found 1274.38.

UV-vis ($CHCl_3$; λ_{max}, nm (log ε)): 294 (4.71), 346 (4.74), 389 (4.82), 441 (5.67), 547 (4.60), 578sh (4.19).

5c

^{1}H NMR ($CDCl_3$; δ, ppm; J, Hz): 8.82 (d, 2H, ^3J = 4.9, H_β), 8.75 (d, 2H, ^3J = 4.9, H_β), 8.71 (s, 2H, H_β), 7.89 (d, 4H, ^3J = 8.3, $CH_{o\text{-}Ar}$), 7.81 (d, 4H, ^3J = 8.2, $CH_{o\text{-}Ar}$), 7.36 (d, 4H, ^3J = 8.3, o-CH), 7.20 (d, 8H, ^3J = 8.2, $CH_{m\text{-}Ar}$), 6.70 (d, 4H, ^3J = 8.3, m-CH), 4.91 (br.s, 2H, OH), 4.25–4.18 (m, 8H, CH_2O), 2.00 (quint, 4H, ^3J = 6.7, CH_2), 1.93 (quint, 4H, ^3J = 6.7, CH_2), 1.70 (sext, 4H, ^3J = 7.4, CH_2), 1.64 (sext, 4H, ^3J = 7.5, CH_2), 1.12 (t, 6H, ^3J = 7.4, CH_3), 1.08 (t, 6H, ^3J = 7.4, CH_3).

^{13}C NMR ($CDCl_3$; δ, ppm): 159.13, 159.09, 156.05, 148.13, 147.12, 144.13, 142.46, 141.62, 134.61, 134.22, 133.28, 132.71, 132.69, 132.63, 132.49, 132.15, 131.74, 131.42, 120.19, 116.15, 114.71, 113.07, 113.02, 68.00, 67.95, 31.77, 31.53, 19.57, 19.41, 14.06, 13.96.

MALDI-TOF MS: m/z calcd for $C_{74}H_{68}N_6NiO_6$ $[M]^+$ 1194.46, found 1194.39.

UV-vis ($CHCl_3$; λ_{max}, nm (log ε)): 293 (4.46), 345 (4.23), 394 (4.57), 441 (5.38), 547 (4.33), 580 (3.92).

5e

^{1}H NMR ($CDCl_3$; δ, ppm; J, Hz): 8.87 (d, 2H, ^3J = 4.9, H_β), 8.77 (d, 2H, ^3J = 4.9, H_β), 8.73 (s, 2H, H_β), 8.25 (d, 4H, ^3J = 7.7, $CH_{o\text{-}Bz}$), 7.90 (d, 4H, ^3J = 8.3, $CH_{o\text{-}Ar}$), 7.84 (d, 4H, ^3J = 8.2, $CH_{o\text{-}Ar}$), 7.67 (t, 2H, ^3J = 7.5, $CH_{p\text{-}Bz}$), 7.59–7.53 (m, 8H, $CH_{m\text{-}Bz}$ + m-CH), 7.21 (t, 8H, ^3J = 8.3, $CH_{m\text{-}Ar}$), 7.18 (d, 4H, ^3J = 8.4, o-CH), 4.21 (t, 8H, ^3J = 6.5, CH_2O), 1.99–1.90 (m, 8H, CH_2), 1.69–1.60 (m, 8H, CH_2), 1.09 (t, 6H, ^3J = 7.4, CH_3), 1.00 (t, 6H, ^3J = 7.4, CH_3).

^{13}C NMR ($CDCl_3$; δ, ppm): 165.01, 159.41, 159.27, 151.60, 147.99, 147.56, 144.25, 142.71, 141.92, 137.19, 134.76, 134.34, 133.78, 133.18, 132.96, 132.72, 132.67, 132.01, 131.97, 131.65, 130.33, 129.79, 128.77, 121.23, 120.45, 116.56, 113.23, 113.21, 68.14, 68.10, 31.93, 31.67, 19.68, 19.55, 14.12, 14.10.

MALDI-TOF MS: m/z calcd for $C_{88}H_{76}N_6NiO_8$ $[M]^+$ 1402.51, found m/z 1402.50.

UV-vis ($CHCl_3$; λ_{max}, nm (log ε)): 341 (4.50), 398 (4.60), 445 (5.34), 546 (4.32), 579 (3.93).

5f

^{1}H NMR ($CDCl_3$; δ, ppm; J, Hz): 8.87 (d, 2H, ^3J = 4.9, H_β), 8.77 (d, 2H, ^3J = 4.9, H_β), 8.73 (s, 2H, H_β), 7.95 (d, 4H, ^3J = 8.0, $CH_{o\text{-}Ar}$), 7.89 (d, 4H, ^3J = 8.1, $CH_{o\text{-}Ar}$), 7.81 (d, 4H, ^3J = 8.0, m-CH), 7.50 (d, 4H, ^3J = 8.0, o-CH), 7.20 (d, 8H, ^3J = 8.1, $CH_{m\text{-}Ar}$), 4.25–4.17 (m, 8H, CH_2O), 3.97 (s, 6H, $COOCH_3$), 2.04 (quint, 4H, ^3J = 8.2, CH_2), 1.94 (quint, 4H, ^3J = 8.2, CH_2), 1.73 (sext, 4H, ^3J = 7.6, CH_2), 1.64 (sext, 4H, ^3J = 7.6, CH_2), 1.15 (t, 6H, ^3J = 7.4, CH_3), 1.09 (t, 6H, ^3J = 7.4, CH_3).

^{13}C NMR ($CDCl_3$; δ, ppm): 166.95, 159.47, 159.29, 147.94, 147.66, 144.20, 143.81, 142.85, 142.08, 134.74, 134.28, 133.05, 132.85, 132.58, 132.53, 132.17, 131.73, 130.75, 130.18, 129.27, 120.59, 116.70, 113.24, 113.19, 68.15, 68.13, 52.25, 31.85, 31.65, 19.70, 19.54, 14.22, 14.09.

MALDI-TOF MS: m/z calcd for $C_{78}H_{72}N_6NiO_8$ $[M]^+$ 1278.48, found 1278.38.

UV-vis ($CHCl_3$; λ_{max}, nm (log ε)): 347 (4.57), 447 (5.26), 550 (4.32), 578sh (3.92).

5g

^{1}H NMR ($CDCl_3$; δ, ppm; J, Hz): 8.85 (d, 2H, ^3J = 4.9, H_β), 8.77 (d, 2H, ^3J = 4.9, H_β), 8.72 (s, 2H, H_β), 7.89 (d, 4H, ^3J = 8.2, $CH_{o\text{-}Ar}$), 7.82 (d, 4H, ^3J = 8.2, $CH_{o\text{-}Ar}$), 7.71 (dd, 4H, $^3J_{H\text{–}P}$ = 12.9, $^3J_{H\text{–}H}$ = 7.9, m-CH), 7.54 (dd, 4H, $^3J_{H\text{–}P}$ = 12.9, $^3J_{H\text{–}H}$ = 7.9, o-CH), 7.22 (d, 4H, ^3J = 8.2, $CH_{m\text{-}Ar}$), 7.20 (d, 4H, ^3J = 8.2, $CH_{m\text{-}Ar}$), 4.25 (t, 4H, ^3J = 6.5, CH_2O), 4.23–4.12 (m, 12H, CH_2O + $CH_3C\underline{H_2}O$), 2.04

(quint, 4H, $^3J = 6.7$, CH_2), 1.94 (quint, 4H, $^3J = 6.7$, CH_2), 1.73 (sext, 4H, $^3J = 7.4$, CH_2), 1.64 (sext, 4H, $^3J = 7.4$, CH_2), 1.39 (t, 12H, $^3J = 7.1$, $C\underline{H}_3CH_2O$), 1.15 (t, 6H, $^3J = 7.4$, CH_3), 1.08 (t, 6H, $^3J = 7.4$, CH_3).

^{13}C NMR ($CDCl_3$; δ, ppm): 159.46, 159.31, 144.24, 143.18 (d, $^3J_{C-P} = 3.3$ Hz), 142.85, 142.07, 134.74, 134.32, 133.08, 132.71, 132.54 (d, $^3J_{C-P} = 2.3$ Hz), 132.20, 131.78, 131.45, 131.38, 130.73, 130.63, 129.45, 128.65, 128.57, 128.20, 120.62, 116.64, 113.26, 113.22, 68.16 (d, $^3J_{C-P} = 4.4$ Hz), 62.35, 62.31, 31.87, 31.65, 19.71, 19.54, 16.55 (d, $^3J_{C-P} = 6.2$ Hz), 14.20, 14.09.

^{31}P NMR ($CDCl_3$; δ, ppm): 18.48 (s).

MALDI-TOF MS: m/z calcd for $C_{82}H_{86}N_6NiO_{10}P_2$ $[M]^+$ 1434.52, found 1434.64.

UV-vis ($CHCl_3$; λ_{max}, nm (log ε)): 346 (4.41), 403 (4.53), 447 (5.13), 550 (4.18), 579sh (3.77).

5h

^{1}H NMR (20% MeOD in $CDCl_3$; δ, ppm; J, Hz): 8.75 (d, 2H, $^3J = 4.9$, H_β), 8.66 (d, 2H, $^3J = 4.9$, H_β), 8.61 (s, 2H, H_β), 7.84 (d, 4H, $^3J = 8.1$, *m*-CH), 7.78 (d, 4H, $^3J = 8.1$,$CH_{o\text{-Ar}}$), 7.71 (d, 4H, $^3J = 8.1$, $CH_{o\text{-Ar}}$), 7.38 (d, 4H, $^3J = 8.0$, *o*-CH), 7.10 (d, 8H, $^3J = 8.5$, $CH_{m\text{-Ar}}$), 4.14–4.08 (m, 8H, CH_2O), 1.91 (quint, 4H, $^3J = 6.4$, CH_2), 1.83 (quint, 4H, $^3J = 6.3$, CH_2), 1.60 (sext, 4H, $^3J = 7.6$, CH_2), 1.53 (sext, 4H, $^3J = 7.6$, CH_2), 1.01 (t, 6H, $^3J = 7.4$, CH_3), 0.97 (t, 6H, $^3J = 7.4$, CH_3).

^{13}C NMR (20% MeOD in $CDCl_3$; δ, ppm): 159.25, 159.07, 147.94, 147.47, 144.05, 143.62, 142.66, 141.90, 134.55, 134.11, 132.83, 132.71, 132.46, 132.39, 131.95, 131.53, 130.49, 129.33, 120.37, 116.51, 113.09, 113.03, 68.09, 68.04, 31.59, 31.42, 19.44, 19.30, 13.81, 13.77.

MALDI-TOF MS: m/z calcd for $C_{76}H_{68}N_6NiO_8$ $[M]^+$ 1250.45, found 1249.90.

UV-vis ($CHCl_3$; λ_{max}, nm (log ε)): 345 (4.51), 448 (5.22), 551 (4.27), 581sh (3.86).

6

^{1}H NMR ($CDCl_3$; δ, ppm; J, Hz): 8.63 (s, 4H, H_β), 8.57 (d, 4H, $^3J = 4.8$, H_β), 8.07 (d, 4H, $^3J = 4.8$, H_β), 7.85 (br.s, 8H, $CH_{o\text{-Ar}}$), 7.32 (br.d, 8H, $^3J = 8.2$, $CH_{o\text{-Ar}}$), 7.18 (d, 8H, $^3J = 8.3$, $CH_{m\text{-Ar}}$), 6.76 (d, 8H, $^3J = 8.3$, $CH_{m\text{-Ar}}$), 4.19 (t, 8H, $^3J = 6.5$, CH_2O), 3.98 (br.t, 8H, $^3J = 6.5$, CH_2O), 1.92 (quint, 8H, $^3J = 6.7$, CH_2), 1.81 (quint, 8H, $^3J = 6.6$, CH_2), 1.63 (sext, 8H, $^3J = 7.4$, CH_2), 1.52 (sext, 8H, $^3J = 7.4$, CH_2), 1.07 (t, 12H, $^3J = 7.4$, CH_3), 0.95 (t, 12H, $^3J = 7.4$, CH_3).

^{13}C NMR ($CDCl_3$; δ, ppm): 159.26, 158.32, 147.60, 145.08, 142.07, 140.76, 134.62, 134.00, 132.76, 132.58, 132.36, 131.98, 131.75, 131.43, 120.38, 115.78, 113.32, 112.95, 68.12, 67.49, 31.77, 31.65, 19.56, 19.54, 14.09, 14.03.

MALDI-TOF MS: m/z calcd for $C_{120}H_{116}N_{10}Ni_2O_8$ $[M^+]$ 1940.77, found 1940.90.

UV-vis ($CHCl_3$; λ_{max}, nm (log ε)): 329 (4.54), 491 (5.12), 424sh, 585 (4.76), 622 (4.25).

8g

^{1}H NMR ($CDCl_3$; δ, ppm; J, Hz): 8.61 (d, 2H, $^3J = 4.8$, H_β), 8.54 (d, 2H, $^3J = 4.8$, H_β), 8.50 (s, 2H, H_β), 7.71 (dd, 4H, $^3J_{H-P} = 12.9$, $^3J_{H-H} = 7.9$, *m*-CH), 7.51 (dd, 4H, $^3J_{H-H} = 8.1$, $^3J_{H-P} = 3.8$ Hz), 7.21 (s, 8H, CH_{Mes}), 4.28–4.13 (m, 8H, CH_2O), 2.65 (s, 6H, *p*-CH_3), 2.57 (s, 6H, *p*-CH_3), 1.87 (s, 12H, *o*-CH_3), 1.75 (s, 12H, *o*-CH_3), 1.40 (t, 12H, $^3J = 7.1$, CH_3).

^{13}C NMR ($CDCl_3$; δ, ppm): 148.26, 146.58, 143.74, 143.33 (d, $^3J_{C-P} = 3.3$), 142.53, 141.93, 139.08, 138.84, 137.95, 137.37, 137.11, 137.01, 132.72, 132.24, 131.39, 131.32 (d, $^3J_{C-P} = 22.1$ Hz), 131.24, 130.81 (d, $^3J_{C-P} = 15.0$), 129.21, 128.02, 127.96, 118.79, 115.27, 62.41 (d, $^3J_{C-P} = 5.5$), 21.68, 21.66, 21.54, 21.53, 16.54 (d, $^3J_{C-P} = 6.3$).

^{31}P NMR ($CDCl_3$; δ, ppm): 18.56 (s).

MALDI-TOF MS: m/z calcd for $C_{78}H_{78}N_6NiO_6P_2$ $[M]^+$ 1314.48, found 1314.24.

UV-vis ($CHCl_3$; λ_{max}, nm (log ε)): 343 (4.77), 396 (4.96), 443 (5.49), 547 (4.59), 581 (4.27).

Synthesis of 9

5a (40 mg, 0.03 mmol) was mixed with 4-methoxycarbonylphenyl pinacolborane (39 mg, 0.15 mmol), CsF (20 mg, 0.129 mmol) and $Pd(Ph_3P)_4$ (4.6 mg, 4 μmol) under argon. Dry DME (8 mL) was added and the mixture was refluxed overnight. The complete conversion of the starting compound was detected by TLC (silica gel, hexane/DCM = 1 : 2), and afterwards the reaction mixture was evaporated to dryness. The residue was applied to a column packed with silica gel in hexane. The column was eluted with hexane/DCM mixtures (0 → 100% of DCM) and the fraction containing **9** was evaporated to provide 37 mg (84%) of the product.

^{1}H NMR ($CDCl_3$; δ, ppm; J, Hz): 8.86 (d, 2H, $^3J = 4.9$, H_β), 8.77 (d, 2H, $^3J = 4.9$, H_β), 8.73 (s, 2H, H_β), 8.12 (d, 4H, $^3J = 8.0$, CH_{Ar}), 7.89 (d, 4H, $^3J = 8.2$, $CH_{o\text{-Ar}}$), 7.81 (d, 4H, $^3J = 8.2$, $CH_{o\text{-Ar}}$), 7.69 (d, 4H, $^3J = 8.1$, CH_{Ar}), 7.57 (d, 4H, $^3J = 8.1$, CH_{Ar}), 7.52 (d, 4H, $^3J = 8.1$, CH_{Ar}), 7.20 (d, 4H, $^3J = 6.3$, $CH_{m\text{-Ar}}$), 7.19 (d, 4H, $^3J = 6.6$, $CH_{m\text{-Ar}}$), 4.19 (t, 4H, $^3J = 6.5$, CH_2O), 4.16 (t, 4H, $^3J = 6.5$, CH_2O), 3.97 (s, 6H, $COOCH_3$), 1.98–1.89 (m, 8H, CH_2), 1.68–1.55 (m, 8H, CH_2), 1.09 (t, 6H, $^3J = 7.4$, CH_3), 1.03 (t, 6H, $^3J = 7.4$, CH_3).

^{13}C NMR ($CDCl_3$; δ, ppm): 167.10, 159.34, 159.26, 148.26, 147.53, 145.09, 144.28, 142.77, 141.98, 139.95, 139.54, 134.75, 134.33, 133.18, 132.95, 132.74, 132.66, 132.03, 131.65, 131.35, 130.25, 129.22, 126.96, 126.69, 120.52, 116.56, 113.22, 113.16, 68.11, 68.07, 52.28, 31.92, 31.65, 19.76, 19.53, 14.14, 14.09.

MALDI-TOF MS: m/z calcd for $C_{90}H_{80}N_6NiO_8$ $[M]^+$ 1430.54, found 1430.66.

UV-vis ($CHCl_3$; λ_{max}, nm (log ε)): 308 (4.56), 345 (4.53), 396 (4.56), 446 (5.26), 550 (4.25), 580 (3.81).

Synthesis of 10

5a (40 mg, 0.03 mmol), $Pd(OAc)_2$ (7.7 mg, 0.03 mmol) and xantphos (35 mg, 0.06 mmol) were mixed under a CO atmosphere, an then BuOH (5 mL) and Et_3N (125 μL, 0.9 mmol) were added. The mixture was heated at 100 °C and bubbled with CO for 3 h. Afterwards, the mixture was cooled to ambient temperature and evaporated to dryness. The residue was applied to a column packed with silica gel in hexane and eluted with hexane/DCM (0 → 100% of DCM) and then with DCM/MeOH (0 → 100% of MeOH) mixtures. The evaporation of the fractions containing **10** provided 22 mg (54%) of the target compound.

^{1}H NMR ($CDCl_3$; δ, ppm; J, Hz): 8.87 (d, 2H, $^3J = 4.9$, H_β), 8.77 (d, 2H, $^3J = 4.9$, H_β), 8.73 (s, 2H, H_β), 7.95 (d, 4H, $^3J = 8.0$, *m*-CH), 7.89 (d, 4H, $^3J = 8.3$, $CH_{o\text{-Ar}}$), 7.82 (d, 4H, $^3J = 8.2$, $CH_{o\text{-Ar}}$), 7.50 (d, 4H, $^3J = 8.1$, *o*-CH), 7.24–7.18 (m, 8H, $CH_{m\text{-Ar}}$), 4.38 (t, 4H, $^3J = 6.7$, CH_2O), 4.27–4.17 (m, 8H, CH_2O), 2.08–2.01 (m, 4H, CH_2), 1.97–1.91 (m, 4H, CH_2), 1.86–1.79 (m, 4H, CH_2), 1.72 (sext, 4H, $^3J = 7.4$, CH_2), 1.64 (sext, 4H, $^3J = 7.6$, CH_2), 1.54 (sext, 4H, $^3J = 7.9$, CH_2), 1.14 (t, 6H, $^3J = 7.4$, CH_3), 1.09 (t, 6H, $^3J = 7.4$, CH_3), 1.04 (t, 6H, $^3J = 7.4$, CH_3).

^{13}C NMR ($CDCl_3$; δ, ppm): 166.59, 159.46, 159.29, 148.02, 147.65, 144.21, 143.75, 142.83, 142.07, 134.75, 134.29, 133.04, 132.88, 132.59, 132.54, 132.16, 131.73, 130.71, 130.56, 129.23, 120.57, 116.69, 113.24, 113.21, 68.15, 68.14, 65.11, 31.84, 31.66, 31.02, 29.85, 19.69, 19.54, 19.46, 14.19, 14.10, 13.95.

MALDI-TOF MS: m/z cacld for $C_{84}H_{84}N_6NiO_8$ $[M]^+$ 1362.57, found 1362.68.

UV-vis ($CHCl_3$; λ_{max}, nm (log ε)): 349 (4.50), 402sh (4.60), 447 (5.21), 550 (4.26), 581 (3.83).

Synthesis of 5g by the phosphonylation of 5a

5a (19 mg, 0.014 mmol), $Pd(OAc)_2$ (1.9 mg, 8 μmol) and dppf (4.7 mg, 8 μmol) were mixed under argon. Toluene (2 mL), EtOH (0.5 mL), diethylphosphite (110 μL, 0.86 mmol) and Et_3N (29 μL, 0.21 mmol) were subsequently added. The resulting solution was refluxed for 20 h. Afterwards, the reaction mixture was evaporated, and the residue was applied to a column packed with silica gel in hexane. The column was eluted with DCM/MeOH mixtures (0 → 20% of MeOH) and the fraction containing **5g** was evaporated to provide 19 mg (95%) of the product.

Synthesis of 11

5a (40 mg, 0.03 mmol), $PdCl_2$dppf (2 mg, 0.003 mmol), KOAc (18 mg, 0.18 mmol) and dipinacoldiborane (23 mg, 0.09 mmol) were mixed under argon, and dioxane (6 mL) was added. The obtained suspension was stirred and heated to 100 °C. The starting material completely dissolved at *ca.* 80 °C. The mixture was heated for 18 h and then cooled to ambient temperature and evaporated to dryness. The residue was applied to a column packed with silica gel in hexane and eluted with hexane/DCM (0 → 100% of DCM) and then DCM/MeOH mixtures (0 → 3% of MeOH) mixtures. The fractions containing **11** were combined, evaporated and repeatedly purified by means of gel-permeation chromatography at Bio-Beads SX-1 with $CHCl_3$/MeOH eluent (2.5% of MeOH) to provide 17 mg (40%) of **11** after evaporation.

^{1}H NMR ($CDCl_3$; δ, ppm; J, Hz): 8.86 (d, 2H, $^3J = 4.9$, H_β), 8.76 (d, 2H, $^3J = 4.9$, H_β), 8.71 (s, 2H, H_β), 7.89 (d, 4H, $^3J = 8.2$, $CH_{o\text{-Ar}}$), 7.81 (d, 4H, $^3J = 8.2$, $CH_{o\text{-Ar}}$), 7.69 (d, 4H, $^3J = 7.7$, *m*-CH), 7.43 (d, 4H, $^3J = 7.7$, *o*-CH), 7.21 (d, 4H, $^3J = 8.4$, $CH_{m\text{-Ar}}$), 7.20 (d, 4H, $^3J = 8.1$, $CH_{m\text{-Ar}}$), 4.24 (t, 4H, $^3J = 6.4$, CH_2O), 4.20 (t, 4H, $^3J = 6.5$, CH_2O), 2.05 (quint, 4H, $^3J = 6.4$, CH_2), 1.94 (quint, 4H, $^3J = 6.3$, CH_2), 1.76 (sext, 4H, $^3J = 7.6$, CH_2), 1.64 (sext, 4H, $^3J = 7.6$, CH_2), 1.39 (s, 24H, CH_{3Pin}), 1.16 (t, 6H, $^3J = 7.4$, CH_3), 1.09 (t, 6H, $^3J = 7.4$, CH_3).

^{13}C NMR ($CDCl_3$; δ, ppm): 159.43, 159.23, 149.09, 147.59, 144.26, 142.64, 142.26, 141.85, 134.74, 134.30, 133.31, 132.88, 132.74, 132.57, 131.93, 131.65, 129.99, 120.35, 116.58, 113.20, 83.91, 68.15, 68.13, 31.93, 31.67, 25.12, 19.70, 19.55, 14.35, 14.10.

MALDI-TOF MS: m/z calcd for $C_{86}H_{90}B_2N_6NiO_8$ $[M]^+$ 1414.64, found 1413.78.

UV-vis ($CHCl_3$; λ_{max}, nm (log ε)): 300 (3.36), 342 (3.43), 394sh (3.50), 443 (4.29), 548 (3.24), 579sh (2.82).

Conflicts of interest

There are no conflicts to declare.

Acknowledgements

The authors are grateful to Russian Foundation for Basic Research and Moscow city Government according to the research project no. 19-33-70036 and Council of the President of Russian Federation for support of young scientists (grant MK-1454.2019.3, synthesis of compounds **4f,g** and **5f,g**) for financial support. The measurements were made at the Shared Facility Centers of the Institute of Physical Chemistry and Electrochemistry RAS.

Notes and references

1 J. Liu, Q. Liang, R. Zhao, S. Lei and W. Hu, *Mater. Chem. Front.*, 2020, **4**, 354–368.
2 D. Ma, J. Li, A. Liu and C. Chen, *Materials*, 2020, **13**, 1734.
3 A. G. Navrotskaya, D. D. Aleksandrova, E. F. Krivoshapkina, M. Sillanpää and P. V. Krivoshapkin, *Front. Chem.*, 2020, **8**, 1–9.
4 O. A. T. Dias, S. Konar, A. L. Leão, W. Yang, J. Tjong and M. Sain, *Front. Chem.*, 2020, **8**, 420.
5 S. W. Shin, J. S. Yuk, S. H. Chun, Y. T. Lim and S. H. Um, *Nano Convergence*, 2020, **7**, 2.
6 C.-X. Yao, N. Zhao, J.-C. Liu, L.-J. Chen, J.-M. Liu, G.-Z. Fang and S. Wang, *Polymers*, 2020, **12**, 691.
7 A. Kayan, *Adv. Compos. Hybrid Mater.*, 2019, **2**, 34–45.
8 N. Aslankoohi, D. Mondal, A. S. Rizkalla and K. Mequanint, *Polymers*, 2019, **11**, 1437.
9 M. J. F. Calvete, G. Piccirillo, C. S. Vinagreiro and M. M. Pereira, *Coord. Chem. Rev.*, 2019, **395**, 63–85.
10 Z. Sun, G. Cui, H. Li, Y. Liu, Y. Tian and S. Yan, *J. Mater. Chem. B*, 2016, **4**, 5194–5216.
11 Ł. Klapiszewski, K. Siwińska-Stefańska and D. Kołodyńska, *Chem. Eng. J.*, 2017, **330**, 518–530.
12 J. Zhang, M. Li, L. Cheng and T. Li, *Polym. Chem.*, 2017, **8**, 6527–6533.
13 A. Wang, J. Zhang, W. Zhao, W. Zhu and Q. Zhong, *J. Alloys Compd.*, 2018, **748**, 929–937.
14 Y. Qiu, Y. Zhang, L. Jin, L. Pan, G. Du, D. Ye and D. Wang, *Org. Chem. Front.*, 2019, **6**, 3420–3427.
15 J. G. Mahy, C. A. Paez, C. Carcel, C. Bied, A. S. Tatton, C. Damblon, B. Heinrichs, M. Wong Chi Man and S. D. Lambert, *J. Photochem. Photobiol., A*, 2019, **373**, 66–76.
16 L. Wang, P. Jin, S. Duan, J. Huang, H. She, Q. Wang and T. An, *Environ. Sci.: Nano*, 2019, **6**, 2652–2661.

17 V. V. Arslanov, M. A. Kalinina, E. V. Ermakova, O. A. Raitman, Y. G. Gorbunova, O. E. Aksyutin, A. G. Ishkov, V. A. Grachev and A. Y. Tsivadze, *Russ. Chem. Rev.*, 2019, **88**, 775–799.
18 S. Supriya, V. S. Shetti and G. Hegde, *New J. Chem.*, 2018, **42**, 12328–12348.
19 L.-Y. Huang, J.-F. Huang, Y. Lei, S. Qin and J.-M. Liu, *Catalysts*, 2020, **10**, 656.
20 J. Min Park, J. H. Lee and W.-D. Jang, *Coord. Chem. Rev.*, 2020, **407**, 213157.
21 W. Gao, J. Tian, Y. Fang, T. Liu, X. Zhang, X. Xu and X. Zhang, *Chemosphere*, 2020, **243**, 125334.
22 T. O. Shekunova, L. A. Lapkina, A. B. Shcherbakov, I. N. Meshkov, V. K. Ivanov, A. Y. Tsivadze and Y. G. Gorbunova, *J. Photochem. Photobiol., A*, 2019, **382**, 111925.
23 I. A. Abdulaeva, K. P. Birin, A. Bessmertnykh-Lemeune, A. Y. Tsivadze and Y. G. Gorbunova, *Coord. Chem. Rev.*, 2020, **407**, 213108.
24 A. V. Shokurov, D. S. Kutsybala, A. G. Martynov, A. V. Bakirov, M. A. Shcherbina, S. N. Chvalun, Y. G. Gorbunova, A. Y. Tsivadze, A. V. Zaytseva, D. Novikov, V. V. Arslanov and S. L. Selektor, *Langmuir*, 2020, **36**, 1423–1429.
25 I. Jiménez-Munguía, A. K. Fedorov, I. A. Abdulaeva, K. P. Birin, Y. A. Ermakov, O. V. Batishchev, Y. G. Gorbunova and V. S. Sokolov, *Biomolecules*, 2019, **9**, 853.
26 Y. Y. Enakieva, A. A. Sinelshchikova, M. S. Grigoriev, V. V. Chernyshev, K. A. Kovalenko, I. A. Stenina, A. B. Yaroslavtsev, Y. G. Gorbunova and A. Y. Tsivadze, *Chem.–Eur. J.*, 2019, **25**, 10552–10556.
27 K. P. Birin, A. I. Poddubnaya, E. V. Isanbaeva, Y. G. Gorbunova and A. Y. Tsivadze, *J. Porphyrins Phthalocyanines*, 2017, **21**, 406–415.
28 I. A. Abdulaeva, D. A. Polivanovskaia, K. P. Birin, Y. G. Gorbunova and A. Y. Tsivadze, *Mendeleev Commun.*, 2020, **30**, 162–164.
29 D. V. Konarev, S. S. Khasanov, M. S. Batov, A. G. Martynov, I. V. Nefedova, Y. G. Gorbunova, A. Otsuka, H. Yamochi, H. Kitagawa and R. N. Lyubovskaya, *Inorg. Chem.*, 2019, **58**, 5058–5068.
30 A. G. Martynov, E. A. Safonova, A. Y. Tsivadze and Y. G. Gorbunova, *Coord. Chem. Rev.*, 2019, **387**, 325–347.
31 M. V. Volostnykh, S. M. Borisov, M. A. Konovalov, A. A. Sinelshchikova, Y. G. Gorbunova, A. Y. Tsivadze, M. Meyer, C. Stern and A. Bessmertnykh-Lemeune, *Dalton Trans.*, 2019, **48**, 8882–8898.
32 K. P. Birin, Y. G. Gorbunova, A. Y. Tsivadze, A. G. Bessmertnykh-Lemeune and R. Guilard, *Eur. J. Org. Chem.*, 2015, **2015**, 5610–5619.
33 K. P. Birin, Y. G. Gorbunova and A. Y. Tsivadze, *RSC Adv.*, 2015, **5**, 67242–67246.
34 I. A. Abdulaeva, K. P. Birin, J. Michalak, A. Romieu, C. Stern, A. Bessmertnykh-Lemeune, R. Guilard, Y. G. Gorbunova and A. Y. Tsivadze, *New J. Chem.*, 2016, **40**, 5758–5774.
35 K. P. Birin, A. I. Poddubnaya, I. A. Abdulaeva, Y. G. Gorbunova and A. Y. Tsivadze, *Dyes Pigm.*, 2018, **156**, 243–249.
36 K. P. Birin, I. A. Abdulaeva, A. I. Poddubnaya, Y. G. Gorbunova and A. Y. Tsivadze, *Dyes Pigm.*, 2020, **181**, 108550.
37 I. A. Abdulaeva, K. P. Birin, A. A. Sinelshchikova, M. S. Grigoriev, K. A. Lyssenko, Y. G. Gorbunova, A. Y. Tsivadze and A. Bessmertnykh-Lemeune, *CrystEngComm*, 2019, **21**, 1488–1498.
38 I. A. Abdulaeva, K. P. Birin, Y. G. Gorbunova, A. Y. Tsivadze and A. Bessmertnykh-Lemeune, *J. Porphyrins Phthalocyanines*, 2018, **22**, 619–631.
39 K. P. Birin, Y. G. Gorbunova and A. Y. Tsivadze, *Dalton Trans.*, 2011, **40**, 11539.
40 K. P. Birin, A. I. Poddubnaya, Y. G. Gorbunova and A. Y. Tsivadze, *Macroheterocycles*, 2017, **10**, 514–515.
41 M. J. Crossley, L. G. King, I. A. Newsom and C. S. Sheehan, *J. Chem. Soc., Perkin Trans. 1*, 1996, 2675–2684.
42 K. P. Birin, I. A. Abdulaeva, D. A. Polivanovskaia, A. A. Sinelschikova, L. I. Demina, A. E. Baranchikov, Y. G. Gorbunova and A. Y. Tsivadze, *Russ. J. Inorg. Chem.*, 2021, DOI: 10.31857/S0044457X21020021.
43 E. V. Vinogradova, Y. Y. Enakieva, S. E. Nefedov, K. P. Birin, A. Y. Tsivadze, Y. G. Gorbunova, A. G. Bessmertnykh Lemeune, C. Stern and R. Guilard, *Chem.–Eur. J.*, 2012, **18**, 15092–15104.
44 T. Hirao, T. Masunaga, Y. Ohshiro and T. Agawa, *Synthesis*, 1981, **1981**, 56–57.
45 W. L. F. Armarego and C. L. L. Chai, *Purification of laboratory chemicals*, Elsevier/Butterworth-Heinemann, 2009.
46 M. Lo, J.-F. Lefebvre, D. Leclercq, A. van der Lee and S. Richeter, *Org. Lett.*, 2011, **13**, 3110–3113.
47 M. Morisue, N. Haruta, D. Kalita and Y. Kobuke, *Chem.–Eur. J.*, 2006, **12**, 8123–8135.